Original Contribution

Journal of Cosmetic Dermatology, **0**, 1–9

Sclareol isolated from *Salvia officinalis* improves facial wrinkles via an antiphotoaging mechanism

Ji-Eun Park, MD,[1] Kyung-Eun Lee, MD,[1] Eunsun Jung, MD,[2] Seunghyun Kang, PhD,[1] & Youn Joon Kim, MD[1]

[1]*COSMAX R&I Center, Seongnam-si, Gyeonggi-do, Korea*
[2]*Biospectrum Life Science Institute, Jeju Island, Korea*

Summary

Background Ultraviolet (UV) irradiation triggers skin photoaging processes, which disrupt the normal three-dimensional integrity of skin. UV-induced oxidative stress, both directly and indirectly, stimulates complex signaling pathways. UV radiation activates skin cell surface receptors on a molecular level and triggers severe changes in extracellular matrix (ECM) proteins, resulting in skin photoaging.
Aims Sclareol isolated from *Salvia officinalis* is widely used as a fragrance material. Sclareol is known to exert various biological activities, but its antiphotoaging effect has not been elucidated to date. Therefore, we evaluated wrinkle improvement efficacy of sclareol.
Methods Human dermal fibroblast cell line (Hs68) and a reconstructed human epidermis (RHE) model were used to evaluate the antiphotoaging effect of sclareol *in vitro*. A clinical study treated with 0.02% sclareol-containing cream was conducted to identify the ability of sclareol to improve wrinkles.
Results First, sclareol enhanced cellular proliferation and blocked UVB-induced cell death. Sclareol inhibited the UVB-induced mRNA expression of matrix metalloproteinases (MMPs) by regulating the protein expression of AP-1 constituents. In RHE model, sclareol recovered the UVB-induced decrease in epidermal thickness and the expression of proliferating cell nuclear antigen (PCNA). In clinical trial, visually assessed changes and several wrinkle parameters were considered to be statistically different between the test and control groups at 12 weeks.
Conclusions In this study, sclareol inhibited various photoaging phenomena in human fibroblasts and RHE model. In addition, sclareol-containing cream improved wrinkles in a clinical trial. Taken together, sclareol alleviates facial wrinkle formation via an antiphotoaging mechanism and may be an effective candidate ingredient.

Keywords: sclareol, photoaging, fibroblast, skin equivalent, facial lines

Introduction

Human skin acts as a defense barrier between internal organs and various external stimuli. However, diverse stimuli in the external environment can easily attack

Correspondence: Seunghyun Kang, COSMAX R&I Center, #902, Pangyo inno valley E, 255, Pangyo-ro, Bundang-gu, Seongnam-si, Gyeongi-do, Korea. E-mail: shyunk@cosmax.com

Accepted for publication May 9, 2016

human skin to result in skin aging. Normally, skin aging is divided into two major processes: intrinsic aging and extrinsic aging. Intrinsic aging, also referred to as chronological aging, is caused by the passage of time. Conversely, extrinsic aging is due to extrinsic factors, especially ultraviolet (UV) light. Therefore, extrinsic skin aging is also referred to as skin photoaging.[1] Clinically, intrinsic skin aging is characterized by an increase in the number of senescent cells, fine wrinkles, pallor, and laxity skin. However, extrinsic aging is associated with coarse and deep wrinkles, mottled pigmentation, dryness, sallowness, severe atrophy, solar elastosis, and increased inflammatory responses.[2]

When human skin is chronically exposed to UV radiation, the generation of reactive oxygen species (ROS) is triggered, leading to skin cancer and other photoaging symptoms.[3] UV-induced ROS incapacitate antioxidant defense mechanisms in the skin, and this oxidative damage to cell components, including nucleotides, proteins, and lipids, ultimately causes apoptotic or necrotic cell death. UV-induced oxidative stress both directly and indirectly stimulates complex signaling pathways. *In vitro*, UV light activates various cell surface receptors of skin keratinocytes and fibroblasts on a molecular level and triggers severe changes in extracellular matrix (ECM) proteins, resulting in collagen degradation.[4] Two major processes cause UV-induced collagen changes: the activation of collagen breakdown and the inhibition of collagen synthesis. Collagen breakdown is principally the result of increased matrix metalloproteinases (MMPs) production, especially MMP-1, MMP-3, and MMP-9, which stimulate disorganized, fragmented collagen distribution. Conversely, the inhibition of collagen synthesis reduces the collagen content in the dermis.[5]

Sclareol (Fig. 1), which is isolated from *Salvia officinalis*, is widely used in the food and cosmetic industries as a fragrance.[6] Sclareol has been known to have many biological activities, such as antioxidation, antifungal, anticancer, antimicrobial, anti-inflammatory, and anticholinesterase activity.[7–11] However, the ability of sclareol to inhibit skin photoaging has not yet been reported. Therefore, the efficacy of sclareol to inhibit UVB-induced photoaging in a human dermal fibroblast cell line (Hs68) and a reconstructed human epidermis 3D skin model (RHE) was evaluated in this study. In addition, a clinical study was performed with 0.02% sclareol-containing cream to verify the wrinkle improvement effect of sclaerol.

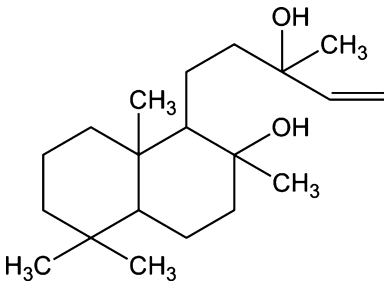

Figure 1 Chemical structure of sclareol.

Materials and methods

Materials

Dulbecco's modified Eagle's medium (DMEM), fetal bovine serum (FBS), and antibiotic/antimycotic solution (AA) were purchased from Thermo Scientific, Waltham, MA, USA. Dulbecco's phosphate-buffered saline (DPBS) from Welgene, Korea, was used to rinse the cells. Tetrazolium dye 3-(4,5-dimethylthiazol-2-yl)-2,5-diphenyltetrazolium bromide (MTT) solution (Sigma-Aldrich, St. Louis, MO, USA) was used to measure the cell viability. Dimethyl sulfoxide (DMSO) was purchased from Samchen chemicals, Pyeongtaek, Korea. RNA iso-solution for RNA isolation was obtained from Takara Bio, Shiga, Japan. RIPA buffer and 10% SDS gels for Western blot analysis were purchased from Sigma-Aldrich and Bio-Rad laboratories (Hercules, CA, USA), respectively. All RHE 3D skin tissue fixation, embedding, staining, and histochemical products were purchased from Sigma-Aldrich and Vector laboratories (Burlingame, CA, USA).

Cell culture and UVB irradiation

The human dermal fibroblast (Hs68) cell line was purchased from the American Type Culture Collection (Menassas, VA, USA). DMEM containing 5% of antibiotic/antimycotic solution and 10% of FBS was used as a complete culture medium. After the Hs68 fibroblasts reached 80% confluence, the cells were rinsed with DPBS and then exposed to a 15 mJ/cm^2 dose of UVB irradiation supplied by a CL-1000M UV Crosslinker (UVP, Upland, CA, USA) at a wavelength of 302 nm to induce photoaging responses. After UVB exposure, the cells were treated with serum-free DMEM or DMEM containing sclareol (1, 5, or 10 μM).

Cell viability test

Fibroblasts (2×10^4) were seeded on a 96-well plate to measure cell viability. The cells were treated with UVB irradiation for 24 h (the controls were not irradiated). The cells were then rinsed with DPBS and

treated with 0.5 mg/mL of MTT solution for an additional 4 h while protected from light. The MTT solution was then removed, and the insoluble formazan crystals were dissolved in DMSO. The absorbance was measured by ELISA spectrophotometry (SpectraMax 190; Molecular devices, CA, USA) at 570 nm.

Real-time reverse transcriptase–polymerase chain reaction (RT-PCR)

The total RNA from Hs68 fibroblasts was isolated using RNAiso reagent according to the recommended protocol. Complementary DNAs, polymerized from the isolated total RNAs using C1000 Touch Thermal Cycler (Bio-Rad), were used as templates for quantitative real-time PCR. The real-time PCR process was performed on a StepOnePlus Real-Time PCR System (Life technologies, Carlsbad, CA, USA).

Western blot analysis

Hs68 fibroblasts were lysed in RIPA lysis buffer, and the protein concentrations were quantified with a Bradford assay. The total protein samples (20 μg each) were separated by 10% SDS gel electrophoresis and transferred to a poly-vinyl difluoride (PVDF) membrane. c-Jun, p-c-Jun, c-Fos, and α-tubulin primary antibodies (Abcam, Cambridge, MA, USA) were used to detect the target proteins on the membrane with a horseradish peroxidase-linked secondary antibody (Bethyl Laboratories, Inc., Montgomery, TX, USA). The blotted antibody signals were detected with ECL detection solution (Thermo Scientific) and visualized with the G:BOX Image Analysis System (Syngene, Cambridge, UK).

3D skin model and UVB irradiation

A 3D RHE model (EpiSkin, Lyon, France) was purchased from SkinEthic to evaluate the antiphotoaging effect of sclareol. The 3D skins were exposed three times to 40 mJ/cm^2 UVB irradiation at 4 h intervals and incubated for an additional 72 h with serum-free medium or sclareol-containing medium (1 or 10 μM). After 72 h, the 3D skin tissues were rapidly fixed in 10% formaldehyde solution and embedded in paraffin blocks for the subsequent experiments.

Hematoxylin and eosin staining and epidermal thickness measurement

Five-micrometer paraffin-embedded 3D skin tissue sections were deparaffinized and rehydrated with xylene and ethanol. First, the sections were stained with hematoxylin to visualize the nuclei in purple. The sections were then stained with eosin to classify the cytosolic area in red. The stained sections were observed under a light microscope (CKX41; Olympus, Tokyo, Japan), and photographs were taken. The epidermal thickness of the skin tissues was measured on the photographs using a tool in the iSolution Lite software (IMT i-Solution Inc., Burlington, ON, Canada).

Immunohistochemistry (IHC)

The deparaffinized and rehydrated paraffin-embedded skin sections were incubated with proliferating cell nuclear antigen (PCNA) primary antibody. Following anti-PCNA incubation, the skin sections were incubated with biotinylated rabbit anti-goat antibody and subsequently incubated with avidin/biotinylated peroxidase complex. The bound antibody was detected with a DAB peroxidase substrate solution and appeared brown. Stained skin sections were observed and photographed under the light microscope.

Clinical trial

A clinical trial of 20 women aged between 39 and 54 years (average age of 45.75 ± 4.29) was conducted at the DERMAPRO skin research center in Korea (Trial code: DEF-HSW1T001(3)-14056). Subjects were randomized into a parallel-test group and applied 0.02% sclareol-containing cream every day and night for 12 weeks. Skin photographs were taken, and both sides of the crow's feet area were visually assessed using the VISIA®-CR facial skin imaging system (Canfield Scientific, Parsippany-Troy Hills, NJ, USA). The wrinkle parameters were analyzed using Skin Visioline® VL650 (Courage & Khazaka, Koln, Germany). Five wrinkle parameters, the total wrinkle area, percentage of wrinkle area, total length, wrinkle depth, and maximum wrinkle depth, were automatically evaluated by the Visioline software using replicas of the crow's feet areas of all subjects.

Statistical analysis

The *in vitro* data are expressed as the mean ± standard deviation (SD) of at least three independent experiments. All data were compared with a *t*-test. The statistical significance of differences observed in the clinical test was analyzed by applying repeated-measures ANOVA using the SPSS Package Program (IBM, Armonk, NY, USA). *P*-values <0.05 were considered to

be statistically significant and were marked as follows: $^{\#\#}P < 0.01$ (compared to (−) control), $^{*}P < 0.05$, and $^{**}P < 0.01$ (compared to UVB control).

Results

Sclareol increases cellular proliferation in both normal and UVB-exposed skin fibroblasts

To evaluate the ability of sclareol to stimulate cell proliferation, we first performed an MTT assay using a human dermal fibroblast cell line (Hs68). Both normal Hs68 cells and UVB-exposed (15 mJ/cm^2) Hs68 cells were treated with different concentrations of sclareol (1, 5, or 10 μM) for 24 h. In result, sclareol gradually increased the number of nonirradiated cells in a dose-dependent manner (Fig. 2a). Additionally, after 15 mJ/cm^2 of UVB irradiation, which diminished the cell viability almost at 70%, sclareol effectively restored the cell viability to a level above 100% at a concentration of 10 μM (Fig. 2b).

Sclareol inhibits MMP expression via the attenuation of AP-1 activation

UVB irradiation triggered the expression of MMPs, especially MMP-1, MMP-3, and MMP-9, which are precisely associated with photoaging regulation. These UVB-induced mRNA levels of MMPs were significantly reduced after sclareol treatment (Fig. 3a). As one of the most important biomarkers used in antiphotoaging strategies, the amount of MMP-1 protein secretion was evaluated additionally. In result, MMP-1 secretion significantly increased after UVB irradiation, but sclareol significantly eliminated this increase in a dose-dependent manner (Fig. 3b).

Subsequently, the protein levels of AP-1 transcription factors, including c-Jun and c-Fos, which stimulate MMP production, were examined with a Western blot analysis. UVB irradiation increased the total protein levels of phospho-c-Jun, c-Jun, and c-Fos, but sclareol treatment dose dependently decreased these levels (Fig. 3c).

Sclareol alleviates UVB-induced epidermal damage in human skin equivalent model

To estimate the change in the epidermal thickness after UVB irradiation in the presence and absence of sclareol, RHE tissues were stained with hematoxylin and eosin. Except for the stratum corneum, the three layers of the epidermis, that is, the stratum basale, stratum spinosum, and stratum granulosum, were stained with hematoxylin to identify the nucleus-containing part of the epidermis. The epidermal thickness of the RHE (except stratum corneum) slightly decreased in the UVB

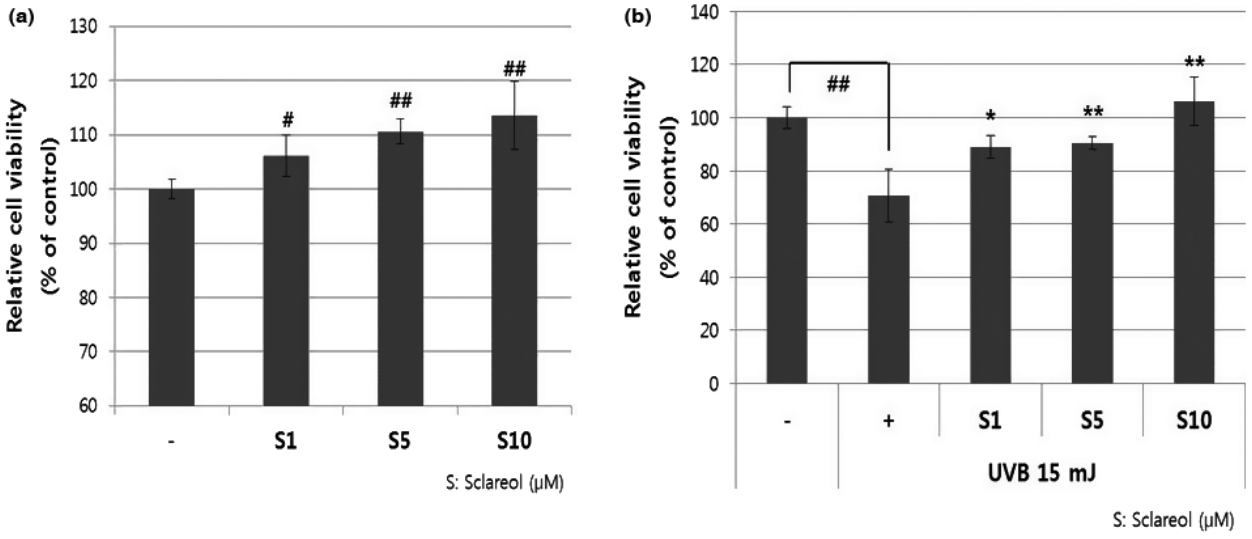

Figure 2 Cellular proliferation in both normal and UVB-exposed Hs68 fibroblasts Relative cell proliferation rate of human dermal fibroblasts (Hs68) was evaluated by MTT assay. (a) Normal Hs68 fibroblasts were treated with various concentrations of sclareol (1, 5, or 10 μM). (b) Sclareol was administered after 15 mJ/cm^2 UVB irradiation. All data were averaged after triplicate independent experiments. (−): non-UVB control, (+): UVB-treated control. $^{\#\#}P < 0.01$ (compared to (−) control), $^{*}P < 0.05$ and $^{**}P < 0.01$ (compared to UVB control).

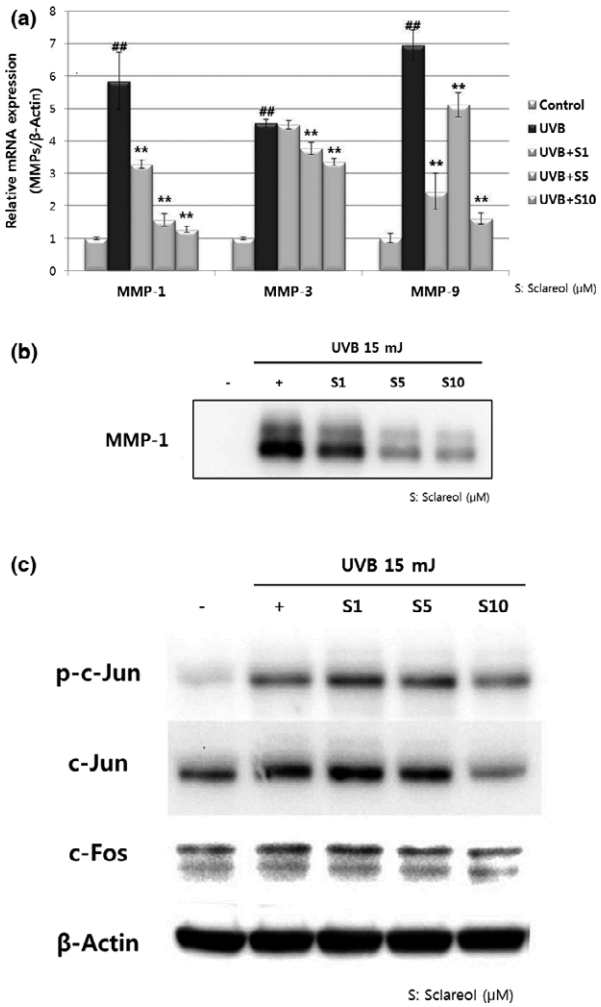

Figure 3 Changes in MMP expression and AP-1 activation on sclareol-treated Hs68 fibroblasts (a) mRNA expression of MMP-1, MMP-3, and MMP-9 was evaluated by real-time RT-PCR. All data were averaged after triplicate independent experiments. $^{\#\#}P < 0.01$ (compared to (−) control), $^{*}P < 0.05$, and $^{**}P < 0.01$ (compared to UVB control). (b) Secreted MMP-1 expression was identified by Western blot analysis using cell medium. Hs68 cells were treated with sclareol after UVB irradiation for 24 h. (c) Protein expression of AP-1 constituents (p-c-Jun, c-Jun, and c-Fos) was also confirmed by Western blot analysis. Equal amount of protein loading was confirmed by β-actin. (−): non-UVB control, (+): UVB-treated control.

control model, but the sclareol-treated model showed an almost intact and fully recovered epidermal thickness. Conversely, the thickness of stratum corneum followed an opposing trend: It was thickened in the UVB control model but thinner in sclareol-treated model (Fig. 4a,b).

Next, proliferating cell nuclear antigen (PCNA), which is only expressed in proliferating cells, was stained using an immunohistochemical method. Large numbers of PCNA-positive cells were observed in the control model, but the number of PCNA-expressing cells was considerably decreased in the UVB-irradiated model. Sclareol treatment upregulated the number of PCNA-positive cells (Fig. 4c,d).

Sclareol improves facial wrinkles in a clinical trial

Visually assessed changes significantly differed between the test group and the control group at 12 weeks (Fig. 5a,b). In addition, skin wrinkle parameters were analyzed with a skin replica analysis. Among the various wrinkle parameters, the total wrinkle area, percent of wrinkle area, and total length significantly differed between the control and test groups (Table 1).

Discussion

Solar UV light produces two opposite effects in humans. It positively affects human health because it is essential for vitamin D synthesis. However, it can be a potent carcinogen, causing skin photoaging or even skin cancer.[12] UV light is split into three subtypes depending on the wavelength: UVA (320–400 nm), UVB (280–320 nm), and UVC (200–280 nm). Because UVC radiation is predominantly absorbed by the ozone layer, UVA and UVB are major UV sources that mainly affect the human epidermis and dermis, contributing to skin photodamage.[4] Many aspects of skin photoaging, especially epidermal features, are principally associated with UVB irradiation.[13] In addition, even though UVB radiation is less abundant than UVA radiation, UVB has more energy and power to induce photoaging and skin cancer.[14] Therefore, we utilized a UVB source in the present study to induce skin photoaging.

Acute and chronic UV irradiation triggers severe skin photoaging processes, which directly disrupt the normal three-dimensional integrity of skin. UV irradiation activates the expression of MMPs in human skin, which degrade the ECM component and reduce collagen production, leading to the impairment of skin resiliency and structural integrity.[5] MMPs are family of zinc-containing proteinases that includes 25 members. Depending on their substrate specificities and whether they are bound to cell membranes or secreted as soluble proteins, MMPs are categorized as collagenases, gelatinases, stromelysins, and membrane-type MMPs (MT-MMPs). Among the 19 MMP members that are expressed in normal human skin, UV irradiation mainly triggers the expression of three MMPs: MMP-1 (interstitial collagenase), MMP-3 (stromelysin-1), and

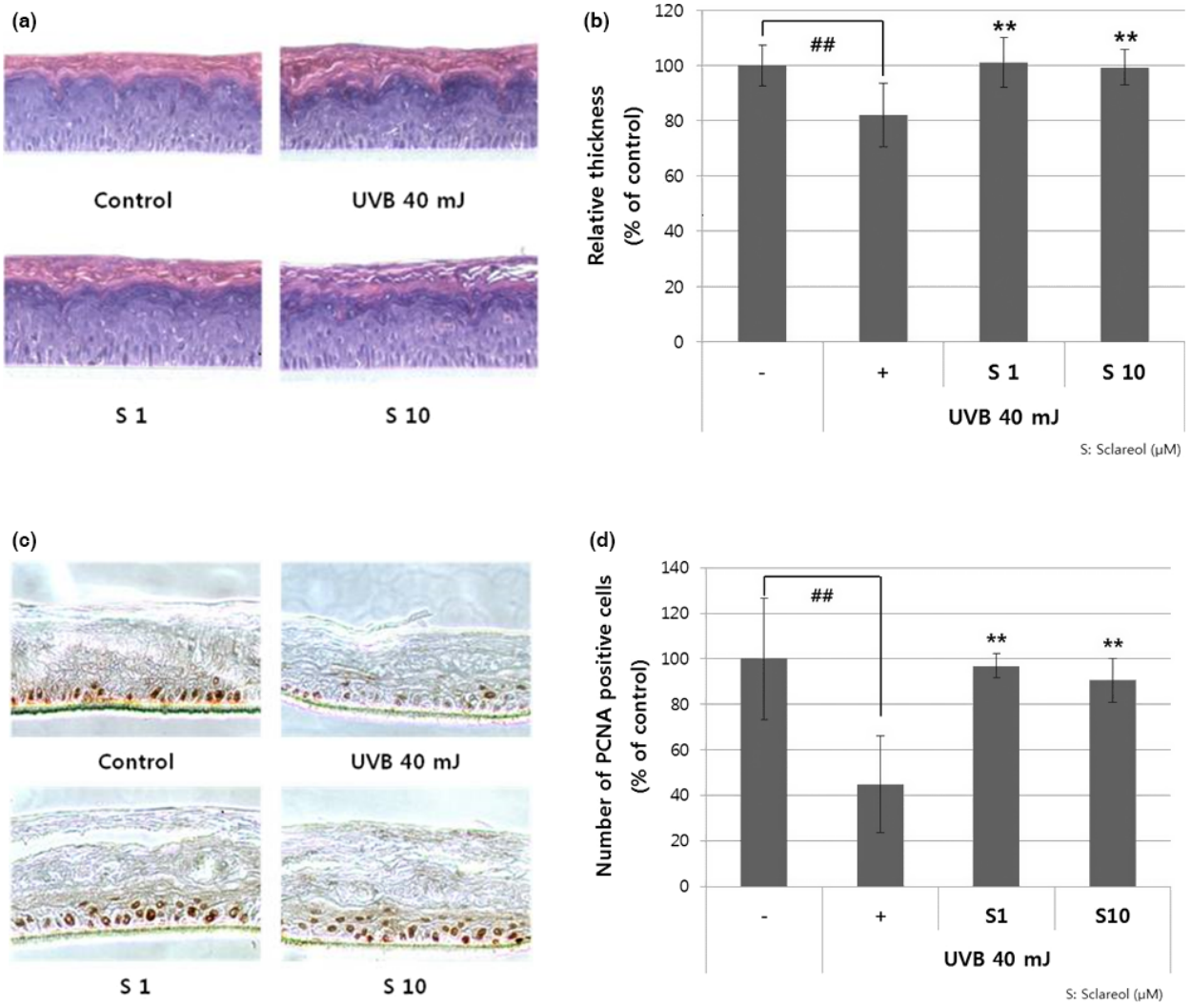

Figure 4 Alterations on UVB-induced epidermal damage in human skin equivalent model 3D reconstructed human epidermis model (EpiSkin™) was exposed to 40 mJ/cm^2 of UVB three times and incubated for 72 h in sclareol-containing culture medium. (a) The 3D skin tissues were stained with H&E. (b) Changes in epidermal thickness were evaluated by measuring the epidermal height of the 3D skin model (except the height of stratum corneum). (c) PCNA expression was identified by immunohistochemical analysis. (d) PCNA-positive cells were counted on randomized photographs, four pictures per group. (−): non-UVB control, (+): UVB-treated control.

MMP-9 (92-kD gelatinase).[3] When the skin is exposed to UV radiation, elevated levels of MMP-1 initially degrade type I and type III collagens in the dermis. Sequentially, MMP-9 further cuts collagen fiber into collagen fragments which are generated by collagenases, while MMP-3 concurrently activates and regulates proMMP-1 and MMP-9.[15] In the present study, we found that sclareol significantly inhibited all three types of MMP expression (Fig. 3a,b). However, sclareol did not affect procollagen biosynthesis sufficiently (data not shown), suggesting that sclareol can effectively alleviate UVB-induced collagen changes, particularly inhibit the breakdown of collagens by MMPs. Principally, UVB upregulates MMP expression by activating the activator protein-1 (AP-1) transcription factor in human dermal fibroblasts.[16] AP-1 is a major regulatory protein involved in cell transformation, growth, differentiation, and apoptosis. AP-1 is also involved in immune responses and inflammatory reactions. Here, sclareol inhibited AP-1 in Hs68 fibroblasts following the inhibition of MMPs (Fig. 3c). These results show that MMP suppression by sclareol is a consequence of AP-1 downregulation.

To date, large numbers of *in vitro* alternative test methods have been developed as substitutes for *in vivo* animal tests in the cosmetic industry. Various

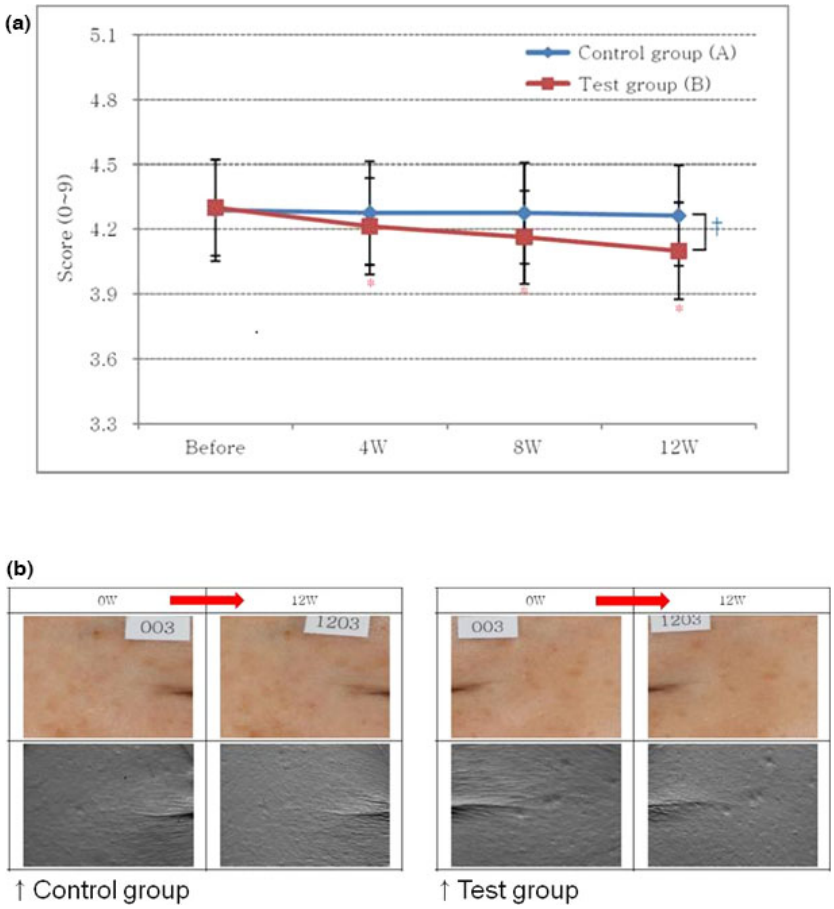

Figure 5 Facial wrinkle assessment in a clinical trial A clinical trial of 20 women was performed with 0.2% sclareol-containing cream for 12 weeks. (a) Changes on both sides of the crow's feet area were visually assessed at 0 (baseline), 4, 8, and 12 weeks. (b) Wrinkle status was measured with the VISIA® CR facial skin imaging system, and skin replicas were analyzed using Visioline® VL650. Control group had applied cream not containing sclareol, and test group had applied sclareol-containing cream.

Table 1 Statistical analysis of skin wrinkle parameters. Five wrinkle parameters were analyzed with the replica data at 4, 8, and 12 weeks. *P*-values <0.05 were considered to be statistically significant marked with *

Parameter	Week	Type III sum of squares	df	Mean square	F	P- value
Total wrinkle area	4W (Test *vs.* Control)	6.763	1	6.763	7.747	0.012*
	8W (Test *vs.* Control)	10.455	1	10.455	4.342	0.051
	12W (Test *vs.* Control)	14.826	1	14.826	5.207	0.034*
Percent of wrinkle area	4W (Test *vs.* Control)	1.383	1	1.383	7.381	0.014*
	8W (Test *vs.* Control)	2.100	1	2.100	4.394	0.050*
	12W (Test *vs.* Control)	3.160	1	3.160	5.452	0.031*
Total length	4W (Test *vs.* Control)	1.717	1	1.717	0.003	0.955
	8W (Test *vs.* Control)	2020.050	1	2020.050	4.607	0.045*
	12W (Test *vs.* Control)	861.066	1	861.066	1.412	0.249
Wrinkle depth	4W (Test *vs.* Control)	731978.843	1	731978.843	0.067	0.798
	8W (Test *vs.* Control)	5620417.060	I	5620417.060	0.173	0.682
	12W (Test *vs.* Control)	42.544	1	42.544	0.000	0.999
Max. wrinkle depth	4W (Test *vs.* Control)	130.509	1	130.509	0.57	0.814
	8W (Test *vs.* Control)	16.617	1	16.617	0.005	0.946
	I2W (Test *vs.* Control)	1961.586	1	1961.586	0.916	0.351

reconstructed human skin models that imitate the human epidermis or dermis have been utilized. Human skin equivalent models are widely used in the cosmetic industry as an alternative to animal experiments. In this study, we used RHE model to evaluate the antiphotoaging effect of sclareol. In the present study, we used RHE model to evaluate the ability of sclareol to protect skin tissue. As shown in Figure 4a,b, the epidermis of the sclareol-treated RHE was thicker than that of the UVB group. In the same vein, we hypothesized that UVB irradiation may block the proliferation of keratinocytes in the RHE, and detected PCNA-positive cells using immunohistochemical methods. The expression of PCNA in the RHE was significantly increased in the sclareol-treated model, which agrees with the epidermal thickness results (Fig. 4c,d). These findings suggest that the increase in the epidermal thickness due to sclareol is related to increased cell proliferation. As a result, sclareol also possesses positive effect on UVB-induced RHE model *in vitro*.

Finally, clinical assessments were performed at week 0 (baseline), 4, 8, and 12 weeks after the application of 0.02% sclareol-containing cream. Two experimenters visually assessed the skin wrinkles by grading the wrinkle states of the subjects. In the present study, a statistical analysis of the visual assessment showed significant differences between the test and control groups at 12 weeks (Fig. 5a,b). Skin wrinkles were analyzed using replica Visioline® VL650 and five parameters: total wrinkle area, percent of winkle area, total length, wrinkle depth, and maximum wrinkle depth. Three of these five wrinkle parameters (total wrinkle area, percent of wrinkle area, and total length) were significantly reduced in the test group compared with the control group (Table 1). The wrinkle depth and maximum wrinkle depth did not significantly differ between the test and control groups. In addition, none of the subjects exhibited allergic responses throughout the test period, which means sclareol-containing cream is mild and safe.

Most organisms exhibit unique photodamage repair mechanisms in response to UV irradiation. Thus, photoprotection is an exciting field in which candidate compounds for the medical and cosmeceutical industries are being investigated. Principally, MMP inhibitors are considered candidate photoprotection agents, and many antioxidants reportedly also exert strong antiphotoaging activities, such as ascorbic acid, beta-carotene, and green tea.[17–19] Here, sclareol strongly inhibited MMPs while simultaneously exhibiting various other photoaging phenomena. Sclareol is also reported as a strong antioxidant.[11] In addition, sclareol not only showed antiphotoaging efficacy *in vitro*, but also exhibited wrinkle improvement effect in clinical test. Taken together, these findings suggest that sclareol may be an effective cosmetic ingredient to help reducing facial wrinkles.

Acknowledgments

This research was financially supported by the Ministry of Trade, Industry and Energy (MOTIE), and the Jeju Institute for Regional Program Evaluation through the Leading Industry Development for Economic Region (R0001467).

References

1 Naylor EC, Watson REB, Sherratt MJ. Molecular aspects of skin ageing. *Maturitas* 2011; **69**: 249–56.
2 Farage M, Miller KW, Elsner P *et al.* Intrinsic and extrinsic factors in skin ageing: a review. *Int J Cosmet Sci* 2008; **30**: 87–95.
3 Pallela R, Na-Young Y, Kim SK. Anti-photoaging and photoprotective compounds derived from marine organisms. *Mar Drugs* 2010; **8**: 1189–202.
4 Pandel R, Poljšak B, Godic A *et al.* Skin photoaging and the role of antioxidants in its prevention. *ISRN Dermatol* 2013; **2013**: 930164.
5 Quan T, Qin Z, Xia W *et al.* Matrix-degrading metalloproteinases in photoaging. *J Investig Dermatol Symp Proc* 2009; **14**: 20–4.
6 Bhatia SP, McGinty D, Letizia CS *et al.* Fragrance material review on sclareol. *Food Chem Toxicol* 2008; **46**: S270–4.
7 Brûle S, Müller A, Fleming AJ *et al.* The ABC transporter SpTUR2 confers resistance to the antifungal diterpene sclareol. *Plant J* 2002; **30**: 649–62.
8 Mahaira LG, Tsimplouli C, Sakellaridis N *et al.* The labdane diterpene sclareol (labd-14-ene-8, 13-diol) induces apoptosis in human tumor cell lines and suppression of tumor growth in vivo via a p53-independent mechanism of action. *Eur J Pharmacol* 2011; **666**: 173–82.
9 Souza AB, de Souza MGM, Moreira M *et al.* Antimicrobial evaluation of diterpenes from Copaifera langsdorffii oleoresin against periodontal anaerobic bacteria. *Molecules* 2011; **16**: 9611–9.
10 Huang GJ, Pan CH, Wu CH. Sclareol exhibits anti-inflammatory activity in both lipopolysaccharide-stimulated macrophages and the λ-carrageenan-induced paw edema model. *J Nat Prod* 2012; **75**: 54–9.
11 Çulhaoğlu B, Yapar G, Dirmenci T *et al.* Bioactive constituents of Salvia chrysophylla Stapf. *Nat Prod Res* 2013; **27**: 438–47.
12 Biniek K, Levi K, Dauskardt RH. Solar UV radiation reduces the barrier function of human skin. *Proc Natl Acad Sci U S A* 2012; **109**: 17111–6.
13 Gilchrest B. Photoaging. *J Invest Dermatol* 2013; **133**: E2–6.

14 Chiang HM, Chen HC, Lin TJ *et al.* Michelia alba extract attenuates UVB-induced expression of matrix metalloproteinases via MAP kinase pathway in human dermal fibroblasts. *Food Chem Toxicol* 2012; **50**: 4260–9.
15 Xu Y, Fisher GJ. Ultraviolet (UV) light irradiation induced signal transduction in skin photoaging. *J Dermatological Sci Suppl* 2005; **1**: S1–8.
16 Yu BC, Lee DS, Bae SM *et al.* The effect of cilostazol on the expression of matrix metalloproteinase-1 and type I procollagen in ultraviolet-irradiated human dermal fibroblasts. *Life Sci* 2013; **92**: 282–8.
17 Elmore AR. Final report of the safety assessment of L-Ascorbic acid, Calcium Ascorbate, Magnesium Ascorbate, Magnesium Ascorbyl Phosphate, Sodium Ascorbate, and Sodium Ascorbyl Phosphate as used in cosmetics. *Int J Toxicol* 2005; **24**: 51–111.
18 Cho S, Lee DH, Won CH *et al.* Differential effects of low-dose and high-dose beta-carotene supplementation on the signs of photoaging and type I procollagen gene expression in human skin in vivo. *Dermatology* 2010; **221**: 160–71.
19 Janjua R, Munoz C, Gorell E *et al.* A two-year, double-blind, randomized placebo-controlled trial of oral green tea polyphenols on the long-term clinical and histologic appearance of photoaging skin. *Dermatol Surg* 2009; **35**: 1057–65.